J Mater Sci (2009) 44:6333–6337
DOI 10.1007/s10853-009-3872-2

Thermal stability of the optical band gap and structural order in hot-wire-deposited amorphous silicon

C. J. Arendse · G. F. Malgas · T. F. G. Muller · B. A. van Heerden · D. Knoesen

Received: 25 June 2008 / Accepted: 9 September 2009 / Published online: 23 September 2009
© Springer Science+Business Media, LLC 2009

Abstract We report on the thermal stability of the optical band gap and structural disorder in hot-wire-deposited a-Si:H with different atomic hydrogen concentrations. Furthermore, the changes in the structural disorder will be correlated with the changes in the optical band gap. Raman spectroscopy shows evidence that no crystallization is induced at temperatures below 550 °C and that the structural disorder increases upon annealing. The increase in the structural disorder results in a broadening of the valence and conduction band tails, thereby pinning the valence and conduction band edges closer together, resulting in a decrease in the optical band gap. Hydrogen evolution occurs at 400 °C via the release of molecular hydrogen trapped in voids, which results in the blistering of the sample surface.

Introduction

Hydrogenated amorphous silicon (a-Si:H) has proven to be of technological importance in applications such as solar cells, thin film transistors and liquid crystal displays [1–3]. However, a major concern of a-Si:H is the fact that the stability of the material degrades when it is exposed to prolonged sunlight illumination [4]. It has been shown that both the atomic hydrogen concentration and structural disorder in a-Si:H are critical factors which eventually determine the stability of the material [5]. The optical band gap of a-Si:H is one of the most widely studied subjects in solar cell applications, since it is related to the electronic structure of the material and, more importantly, since the efficiency of solar cells made from this material is directly related to it. It is generally accepted that the band gap is dependent on both the hydrogen content and the structural disorder [6–10]. Furthermore, numerous reports have confirmed that the structural and opto-electronic properties of a-Si:H are directly dependent on the deposition parameters used during the deposition of the material. In the case of hot-wire chemical vapour deposition (HWCVD), the structural and opto-electronic properties are specifically dependent on the substrate temperature, deposition pressure, gas flow rate and hydrogen dilution [7].

In this contribution, we investigate the relation between the optical band gap and the structural disorder in hot-wire-deposited (HW-deposited) a-Si:H thin films, with different bound hydrogen content in the as-deposited state. The changes in the structural disorder and bound hydrogen content were induced and controlled by post-deposition isochronal annealing. Additionally, the effusion mechanism of hydrogen will be discussed and related to changes in the surface morphology.

C. J. Arendse · T. F. G. Muller · B. A. van Heerden · D. Knoesen
Department of Physics, University of the Western Cape, Private Bag X17, Bellville 7535, South Africa

G. F. Malgas (✉)
National Centre for Nano-Structured Materials, Council for Scientific and Industrial Research, P.O. Box 395, Pretoria 0001, South Africa
e-mail: gmalgas@csir.co.za

Experimental details

The a-Si:H samples were deposited simultaneously on single-side polished ⟨100⟩ crystalline silicon (c-Si) and Corning 7059 substrates by the HWCVD process [11] in an MVSystems® deposition chamber [12, 13], where SiH_4 gas is decomposed by the catalytic action of seven parallel

Table 1 Deposition conditions of the a-Si:H thin films

Sample no.	Substrate temperature (°C)	Deposition pressure (Pa)	Silane flow rate (sccm)	Thickness (nm)
A	330	2	60	257
B	180	8	60	845

tantalum wires at a temperature of 1600 °C. The substrate-to-filament distance and the separation distance between the wires amounted to 18 and 15 mm, respectively. The deposition conditions of the samples are given in Table 1.

Isochronal annealing was performed under high purity, flowing argon gas in a tube furnace. The samples were annealed subsequently at annealing temperatures (T_A) ranging from 150–450 °C in 50 °C increments with a total annealing time of 30 min per annealing temperature. It should be noted that this temperature range excludes the strong hydrogen effusion peak observed at 550 °C in device quality a-Si:H [14]. The ambient temperature at the sample position in the experimental set-up amounted to 21 °C.

Fourier transform infrared spectroscopy (FTIR) measurements were performed in transmission mode on the samples deposited on c-Si, using a Digilab FTS-40 FTIR spectrophotometer equipped with a liquid-nitrogen-cooled HgCdTe detector. The atomic hydrogen content was calculated from the integrated absorption of the rocking modes of $\equiv$Si–H, $(=Si=H_2)_n$ and $-Si\equiv H_3$ using the procedures of Brodsky et al. [15] and proportionality constant proposed by Shanks et al. [16]. The error in the results is estimated to be within 15%. It should be noted that no bound hydrogen was detected by FTIR spectroscopy at annealing temperatures in excess of 400 and 450 °C in sample A and B, respectively.

Raman spectroscopy measurements were performed in reflection mode on the samples deposited on Corning 7059, using the 514.5 nm line of a Spectra Physics Ar^+-ion laser. A detailed description of the Raman experimental set-up is given elsewhere [17]. The transverse-optical peak (TO) in the vibrational density of states of amorphous silicon reflects the degree of disorder in the amorphous network [18].

Optical reflection and transmission measurements were performed in the energy range 1.2–2.4 eV with an energy resolution of 3 meV. These measurements were used to calculate the sample thickness, refractive index and absorption coefficient, using the method proposed by Denton et al. [19]. The thickness of the samples is given in Table 1.

The surface morphology was examined using a Hitachi X650 scanning electron microscope (SEM), equipped with analySIS® imaging software and capable of operating at a maximum accelerating voltage of 40 kV.

Results and discussion

The Raman spectra of samples A and B in the as-deposited and final annealing states are shown in Figs. 1 and 2, respectively. The spectra were normalised to the height of the a-Si TO peak. No emerging c-Si TO peaks are observed at $\sim$520 cm^{-1} before and after annealing, illustrating that no amorphous-to-crystalline phase transitions occur in both samples as annealing progresses. Further annealing of both samples up to 550 °C induces no detectable phase

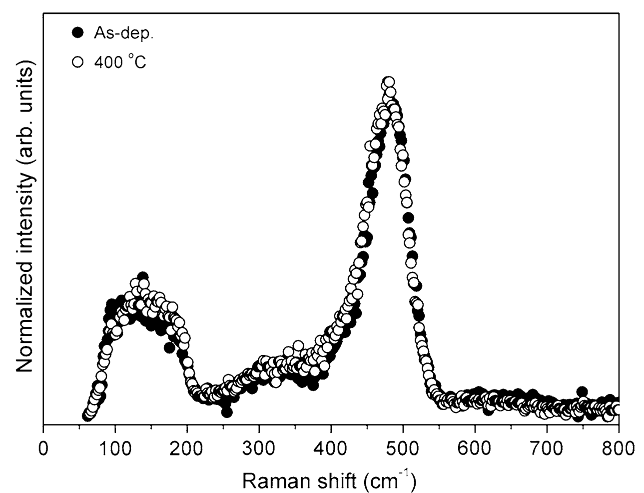

Fig. 1 Raman spectra of sample A in the as-deposited state (*solid circles*) and after annealing at 400 °C (*open circles*)

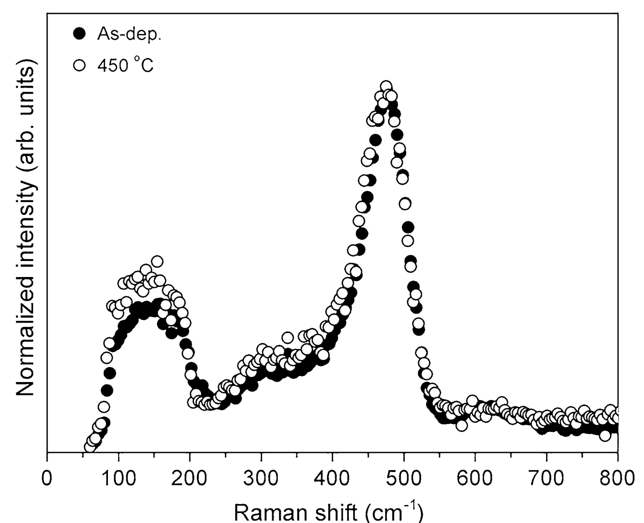

Fig. 2 Raman spectra of sample B in the as-deposited state (*solid circles*) and after annealing at 450 °C (*open circles*)

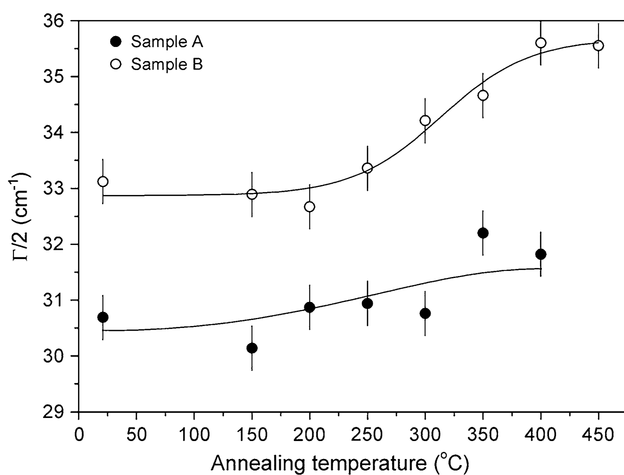

Fig. 3 HWHM of the a-Si TO peak as a function of annealing temperature for sample A (*solid circles*) and sample B (*open circles*)

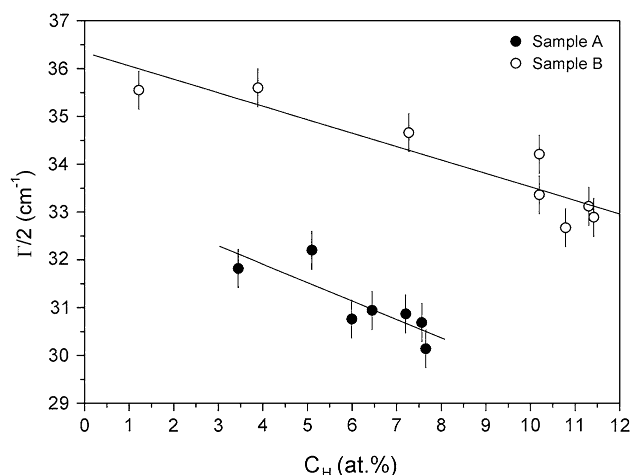

Fig. 4 HWHM of the a-Si TO peak as a function of the hydrogen content for sample A (*solid circles*) and sample B (*open circles*)

transitions. This is consistent with the observations of Spinella et al. [20] who have shown that crystal grain nucleation in a-Si occurs at temperatures above 560 °C.

The plot of the half-width-at-half-maximum (HWHM) of the a-Si TO peak ($\Gamma/2$) as a function of annealing temperature for samples A and B is shown in Fig. 3. There exists a linear relationship between $\Gamma/2$ and the average bond angle variation $\Delta\vartheta_b$ [18]. In the as-deposited state the $\Delta\vartheta_b$ value for samples A and B amounts to 7.28° and 8.03°, respectively. The $\Delta\vartheta_b$ value of sample A is among the lowest determined for device quality HW-deposited a-Si:H [21], illustrating the superior structural quality of this sample. Annealing sample A at temperatures up to 300 °C induces no considerable change in $\Gamma/2$ followed by an increase for $T_A \geq 350$ °C. An increase in $\Gamma/2$ is observed for sample B at $T_A \geq 300$ °C. The increase in $\Gamma/2$ is associated with an increase in the structural disorder, caused by the creation of unterminated Si-dangling bonds, which is illustrated by the reduction in the atomic hydrogen concentration (see Fig. 4). We propose that the atomic hydrogen released from the Si–H_x bonds combine to result in the formation of molecular hydrogen [22], which become trapped inside microvoids.

The optical band gap E_g was determined from the absorption coefficient (α) and the refractive index (n) using the Tauc convention [23], by extrapolating $[\alpha(E)n(E)E]^{1/2}$ to $\alpha(E) = 0$ for $\alpha(E) \geq 10^3$ cm^{-1}. The interference fringes in the optical transmission spectra of thin films can result in an inaccurate Tauc analysis; and therefore both the transmission and reflection spectra, measured simultaneously on the same sample spot, were used throughout the analysis process [19]. The optical band gap as a function of annealing temperature for samples A and B is shown in Fig. 5. After annealing samples A and B at 350 and 300 °C,

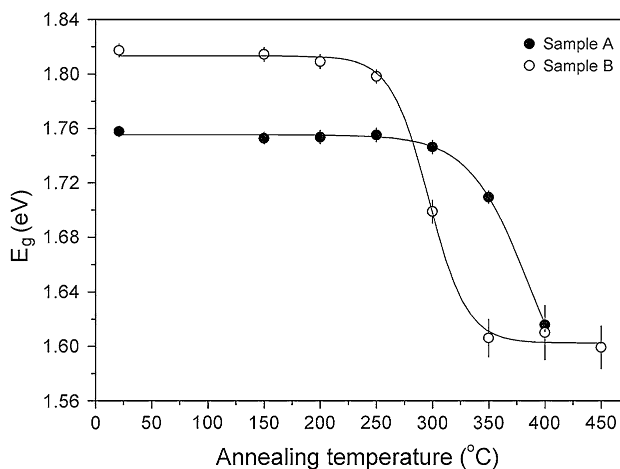

Fig. 5 Optical band gap as a function of annealing temperature for sample A (*solid circles*) and sample B (*open circles*)

respectively, a decrease in E_g is observed. It should be noted that similar trends in the cubic band gap, which assumes linear band edges [24], for samples A and B were observed.

Müller et al. [25] have shown that the slope of the linear fit (B_g) through $[\alpha(E)n(E)E]^{1/2}$ is proportional to the density of states in the valence and conduction band tails. Figure 6 shows the plot of B_g as a function of annealing temperature for samples A and B. Similar trends in E_g and B_g are observed with increasing annealing temperature, suggesting that the decrease in B_g is associated with the broadening of the valence and conduction band tails, thereby pinning the valence and conduction band edges closer together resulting in a reduction in E_g. The broadening of the valence and conduction bands is caused by an increase in the structural disorder, as seen by the increase in $\Gamma/2$ (Fig. 3). Therefore, we conclude that the decrease in the band gap is a direct result of the increase in the structural disorder.

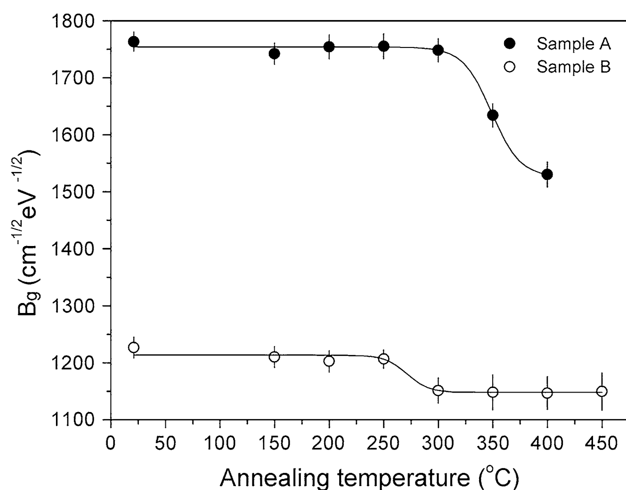

Fig. 6 The slope of the linear fit though $[\alpha(E)n(E)E]^{1/2}$ as a function of annealing temperature for sample A (*solid circles*) and sample B (*open circles*)

A preceding report by our group, which addressed the thermal-induced changes in the defect structure [13], has confirmed that isochronal annealing at temperatures in excess of 150 °C induce a growth in the defect size and defect density, due to the creation and subsequent alignment of unterminated dangling bonds, resulting in the creation of microvoids. The creation of unterminated dangling bonds and the increase in the structural disorder is associated with an increase in the defect states in the band tails and the mid band gap [26], which is synonymous with a reduction in the photoconductivity of a-Si:H [4].

Figure 7 shows a SEM micrograph of the surface of sample B after annealing at 400 °C. Holes with diameters of ~1.5 μm are evident, attributed to the release of molecular hydrogen from the sample. We propose that hydrogen effusion occurs via an accumulation of molecular hydrogen in high-pressure microvoids, which eventually open by explosion and consequently results in the blistering of the surface. Similar changes in the morphology of plasma-deposited a-Si:H have been observed by Rüther et al. [27]. Hydrogen evolution in a-Si:H generally occurs via two processes: a low temperature effusion at 370 °C, attributed to the release of molecular hydrogen through voids or cracks from polysilane-like intergrain material; and an evolution at 550 °C from compact material, dominated by the diffusion of atomic hydrogen [14]. In this instance, the former low temperature mechanism is applicable.

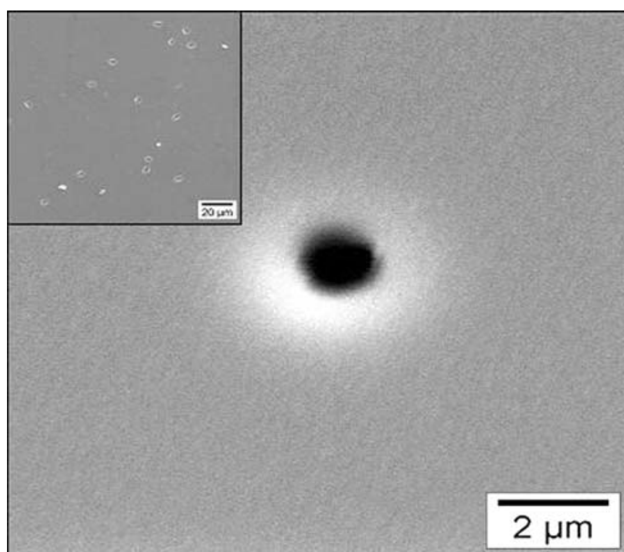

Fig. 7 SEM micrograph of surface of sample B after annealing at 400 °C. The insert is at a lower magnification

Conclusion

Raman spectroscopy and optical measurements were used to correlate changes in the structural disorder and the optical band gap in HW-deposited a-Si:H subjected to isochronal annealing at temperatures ranging from 150 to 450 °C, which excludes the strong hydrogen effusion peak observed around 550 °C in device quality a-Si:H. No crystallization is induced in both samples in this temperature range. The structural properties of sample A, deposited at optimum conditions, remain stable at higher temperatures (300 °C) compared to sample B, which is attributed to its superior structural order and low hydrogen content. The increase in the structural disorder in both samples is ascribed to the creation of unterminated Si-dangling bonds, which consequently results in a reduction in the optical band gap through the broadening of the valence and conduction band tails and the subsequent pinning of the band edges. The low temperature effusion of hydrogen occurs at 400 °C via the release of molecular hydrogen through voids, which results in the creation of holes in the sample surface and the subsequent blistering thereof.

Acknowledgements The authors acknowledge the financial support of the National Research Foundation of South Africa (GUN. 2050646). The authors are especially thankful to Dr. Anke Brockhoff, formerly of the Debye Institute of Utrecht University, for the Raman spectroscopy measurements.

References

1. Madan A, Shaw MP (1988) The physics and applications of amorphous semiconductors. Academic Press, Orlando, FL
2. Chu V, Jarego J, Silva H, Silva T, Reissner M, Brogueira P, Conde JP (1997) Appl Phys Lett 70:2714
3. Meiling H, Schropp REI (1997) Appl Phys Lett 70:2681
4. Staebler DL, Wronski CR (1977) Appl Phys Lett 31:292

5. Street RA, Winer K (1989) Phys Rev B 40:6236
6. Berntsen AJM (1993) PhD thesis, Utrecht University, Utrecht, The Netherlands
7. Feenstra KF, Schropp REI, van der Weg WF (1999) J Appl Phys 85:6843
8. Maessen KHM, Pruppers MJM, Bezemer J, Habraken FHPM, van der Weg WF (1987) Mater Res Soc Symp Proc 95:201
9. Meiling H, van den Boogaard MJ, Schropp REI, Bezemer J, van der Weg WF (1990) Mater Res Soc Symp Proc 192:645
10. Maley N, Lannin JS (1987) Phys Rev B 36:1146
11. Wiesmann H, Ghosh AK, McMahon T, Strongin M (1979) J Appl Phys 50:3752
12. Arendse CJ, Malgas GF, Muller TFG, Knoesen D, Oliphant CJ, Motaung DE, Halindintwali S, Mwakikunga BW (2009) Nanoscale Res Lett 4:307
13. Arendse CJ, Knoesen D, Britton DT (2006) Thin Solid Films 501:92
14. Beyer W, Wagner H (1985) J Non-Cryst Solids 77–78:857
15. Brodsky MH, Cardona M, Cuomo JJ (1977) Phys Rev B 16:3556
16. Shanks H, Fang CJ, Ley L, Cardona M, Desmond FJ, Kalbitzer S (1980) Phys Status Solidi B 100:43
17. Brockhoff AM (2001) PhD thesis, Utrecht University, Utrecht, The Netherlands
18. Beeman D, Tsu R, Thorpe MF (1985) Phys Rev B 32:874
19. Denton RE, Campbell RD, Tomlin SG (1972) J Phys D 5:852
20. Spinella C, Lombardo S, Priolo F (1998) J Appl Phys 84:5383
21. Mahan AH, Williamson DL, Furtak TE (1997) In: Wagner S, Hack M, Schiff EA, Schropp REI, Shimizu I (eds) Amorphous and microcrystalline silicon technology, vol 467. Materials Research Society, Pittsburgh
22. Lucovsky G, Zing Z, Lu Z, Lee DR, Whitten JL (1995) J Non-Cryst Solids 182:90
23. Tauc J (1972) In: Abeles F (ed) Optical properties of solids. North-Holland Publ, Amsterdam
24. Klazes RH, van den Broek MHLM, Bezemer J, Radelaar S (1982) Philos Mag B 45:377
25. Müller G, Mannsperger H, Kalbitzer S (1986) Philos Mag B 53:257
26. Street RA, Knights JC, Biegelsen D (1978) Phys Rev B 18:1880
27. Rüther R, Livingston J (1994) Thin Solid Films 251:30